

# SCIENTIFIC REPORTS



OPEN

## Experimental evidences for reducing Mg activation energy in high Al-content AlGa<sub>N</sub> alloy by Mg<sub>Ga</sub> δ doping in (AlN)<sub>m</sub>/(Ga<sub>N</sub>)<sub>n</sub> superlattice

Received: 03 August 2016  
Accepted: 06 February 2017  
Published: 14 March 2017

Xiao Wang, Wei Wang, Jingli Wang, Hao Wu & Chang Liu

P-type doping in high Al-content AlGa<sub>N</sub> alloys is a main challenge for realizing AlGa<sub>N</sub>-based deep ultraviolet optoelectronics devices. According to the first-principles calculations, Mg activation energy may be reduced so that a high hole concentration can be obtained by introducing nanoscale (AlN)<sub>i</sub>/(Ga<sub>N</sub>)<sub>1</sub> superlattice (SL) in Al<sub>0.83</sub>Ga<sub>0.17</sub>N disorder alloy. In this work, experimental evidences were achieved by analyzing Mg doped high Al-content AlGa<sub>N</sub> alloys and Mg doped AlGa<sub>N</sub> SLs as well as Mg<sub>Ga</sub> δ doped AlGa<sub>N</sub> SLs. Mg acceptor activation energy was significantly reduced from 0.378 to 0.331 eV by using Mg<sub>Ga</sub> δ doping in SLs instead of traditional doping in alloys. This new process was confirmed to be able to realize high p-type doping in high Al-content AlGa<sub>N</sub>.

High Al-content AlGa<sub>N</sub> alloys are ideal materials for deep ultraviolet (DUV)<sup>1</sup> optoelectronic devices due to their large direct band gaps with operating wavelengths from 364 nm down to 200 nm<sup>2-5</sup>. The external quantum efficiency (EQE) of AlGa<sub>N</sub>-based DUV light-emitting diodes (LEDs), however, is as extremely low as 0.1%, which is still a formidable obstacle<sup>6,7</sup>. N-type AlGa<sub>N</sub> can be produced relatively easily<sup>8,9</sup>. The very low p-type doping efficiency in AlGa<sub>N</sub> hinders the further improvement of AlGa<sub>N</sub>-based DUV LEDs. The difficulty to realize p-type doping is related to the high acceptor activation energy ( $E_A$ ), the compensation by nitrogen vacancies, the increased hole scattering, and the limited acceptor solubility<sup>10,11</sup>. For the most widely used p-type dopant of Mg, its  $E_A$  in Al<sub>x</sub>Ga<sub>1-x</sub>N increases monotonically with increasing Al-content from 0.17 eV in GaN to 0.51 eV in AlN<sup>11,12</sup>. This behavior indicates that only a very tiny fraction (~10<sup>-9</sup>) of Mg dopants can be activated in AlN at room temperature<sup>11</sup>. Therefore, decreasing Mg acceptor activation energy is one of the most challenges in AlGa<sub>N</sub>-based DUV optoelectronic devices.

Great efforts have been devoted to improve p-type conduction in group-III nitrides<sup>13-20</sup>. Different from suppressing the charge separation effect in InGa<sub>N</sub>-based devices, polarization doping has been applied to increase the hole concentration in AlGa<sub>N</sub> alloys by ionizing Mg acceptor in the polarization field<sup>13,14</sup>. Alternative acceptor-donor co-doping and non-equilibrium growth with Mg pulse doping and Mg δ-doping have also been developed to reduce the acceptor activation energy, and thus, increase the hole concentration and enhance the p-type conductivity of AlGa<sub>N</sub> alloys<sup>15-20</sup>. So far, most experiments were focused on the p-type conduction of GaN and low Al-content AlGa<sub>N</sub> alloys, but the bottlenecks of the p-type doping in high Al-content AlGa<sub>N</sub> still remain<sup>20-22</sup>.

Many works were concentrated on the doping in the superlattices (SLs)<sup>23-29</sup>, where a periodic oscillation of the valence band edge was created by the valence band discontinuity and innate polarization fields in Mg-doped AlGa<sub>N</sub>/GaN SLs, resulting in the accumulation of holes near the valence band edge close to the Fermi energy forming the so-called two-dimensional (2D) hole gases. In our previous work, we have used Si<sub>Ga</sub> δ doping in Al<sub>0.6</sub>Ga<sub>0.4</sub>N alloys to increase the n-type carrier density<sup>30</sup>. Recent theoretical works predicted that the nanoscale (AlN)<sub>m</sub>/(Ga<sub>N</sub>)<sub>n</sub> (m > n) SL could convert the valence-band maximum (VBM) from the crystal-field split-off hole to heavy hole band, leading to the increase of the transverse electric (TE) polarized light emission efficiency<sup>31,32</sup>.

Key Laboratory of Artificial Micro- and Nano-structures of Ministry of Education, School of Physics and Technology, Wuhan University, Wuhan 430072, China. Correspondence and requests for materials should be addressed to H.W. (email: H.Wu@whu.edu.cn) or C.L. (email: Chang.Liu@whu.edu.cn)

Sample ID	T <sub>Al</sub> (°C)	T <sub>Ga</sub> (°C)	T <sub>substrate</sub> (°C)	T <sub>Mg</sub> (°C)	t <sub>Al</sub> (s)	t <sub>Gap</sub> (s)	t <sub>Ga</sub> (s)	t <sub>Gap</sub> (s)
D1	1260	960	795	340	—	—	—	—
D2	1250	970			—	—	—	—
D3	1260	960			8	—	2	—
D4	1260	960			5	—	5	—
D5	1260	960			8	2	2	3
D6	1260	960			5	2	5	3

**Table 1.** The growth details of all the samples from D1 to D6. Sample D1 and D2 were traditional Mg doped alloys. Sample D3 and D4 were Mg doped SLs. Sample D5 and D6 were Mg<sub>Ga</sub> δ doped SLs. The time “t” inside is the open time in one single loop. “—” means 0 s.

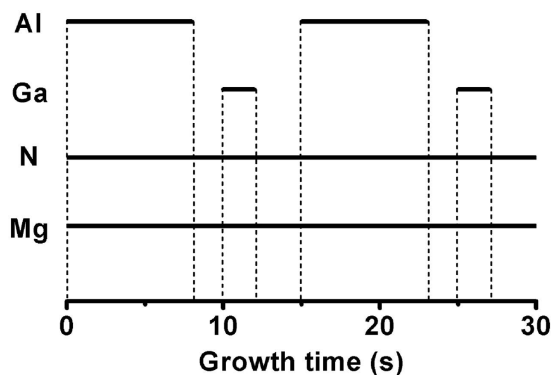


**Figure 1.** Two loops of the growth process of sample D5. The solid and blank lines indicates open and close of the source shutters, respectively.

The influence of the nearest and next-nearest (NN) atoms on Mg electronic structures in nanoscale (AlN)<sub>5</sub>/(GaN)<sub>1</sub> SL substitution for Al<sub>0.83</sub>Ga<sub>0.17</sub>N disorder alloy was theoretically investigated by Zhong *et al.*<sup>1</sup>. The results showed that the E<sub>A</sub> decreases if the NN Ga atom number increased and the Mg-centered tetrahedron volume decreased. In this way, the Mg acceptor activation energy can significantly be reduced to 0.26 eV, very close to that of GaN, in (AlN)<sub>5</sub>/(GaN)<sub>1</sub> SL by Mg<sub>Ga</sub> δ-doping<sup>1</sup>. Recently, improved p-type conductivity was achieved in multi-dimensional Al<sub>0.63</sub>Ga<sub>0.37</sub>N/Al<sub>0.51</sub>Ga<sub>0.49</sub>N SLs<sup>33</sup>. In this work, we use Mg<sub>Ga</sub> δ doping in (AlN)<sub>m</sub>/(GaN)<sub>n</sub> SLs to study Mg acceptor activation energy, aiming to find a proper way to minimize it in high Al-content AlGaN.

## Methods

In this work, traditional Mg doped AlGaN alloys (in which Al, Ga, Mg and N atoms arrived at the substrate at the same time), Mg doped AlGaN SLs and Mg<sub>Ga</sub> δ doped AlGaN SLs were grown on c-plane sapphire substrates by using the radio-frequency plasma-assisted molecular beam epitaxy system (rf-MBE, SVTA 35-V-2). The growth details are shown in Table 1. Sample D1 and D2 were Mg doped AlGaN alloys with traditional doping method. Mg doping was continuously carried out for 30 min. Sample D3 and D4 were Mg doped AlGaN SLs. Mg doping was continuously performed for 10 s at each cycle and the total deposition lasted for 180 cycles. Hence the real Mg doping time was also 30 min. Sample D5 and D6 were Mg<sub>Ga</sub> δ doped AlGaN SLs with a cycle period of 15 s for 180 cycles. Although the cycle period of sample D5 and D6 was 15 s, the effective growth time in a cycle was still kept as 10 s and the total effective growth time was also 30 min. For sample D5, the growth process consisted of two loops as shown in Fig. 1. During the growth of AlGaN thin films, the nitrogen flow rate was set at 2.65 sccm under 375 W rf-plasma power. Prior to the growth, nitridation was performed at 810 °C for 10 min under 500 W rf-plasma power with a nitrogen flow rate of 2.65 sccm. AlGaN films were examined by high-resolution x-ray diffraction (HRXRD, Bede D1) and high-resolution transmission electron microscopy (HRTEM, JEOL JEM 2010 FEF UHR). Ni/Au electrodes (15 nm Ni and 50 nm Au) were made by thermal evaporation with templates of 150 × 150 μm<sup>2</sup> in area. Current versus voltage (I-V) characteristics were measured by using a semiconductor device analyzer (Keithley 4200, Keithley Instruments).

## Results

Figure 2 shows XRD patterns of AlGaN films grown on sapphire substrates. AlGaN (0002) peaks were found between the GaN (0002) peak at 34.543° and AlN (0002) peak at 36.033°. The Al<sub>2</sub>O<sub>3</sub> (0006) peaks were normalized at 41.700°. The full widths at half maximum (FWHM) of the Mg-doped AlGaN (0002) peaks were around 800 arcsec in alloys and 1000 arcsec in SLs. AlGaN peaks were fitted with Gauss model to get more accurate peak information. According to the alloy crystal parameter formula  $c_{\text{Al}_x\text{Ga}_{1-x}\text{N}} = (1-x)c_{\text{GaN}} + xc_{\text{AlN}}$  and Bragg's law  $2d_{\text{hkl}}\sin\theta = n\lambda$  as well as hexagonal interplanar distance formula  $d_{\text{hkl}} = 1/\sqrt{4(h^2 + k^2 + hk)/(3a^2) + l^2/c^2}$ , the compositions of Al<sub>x</sub>Ga<sub>1-x</sub>N thin films were determined by using standard crystal parameter  $c_{\text{GaN}}$  of 0.5189 nm

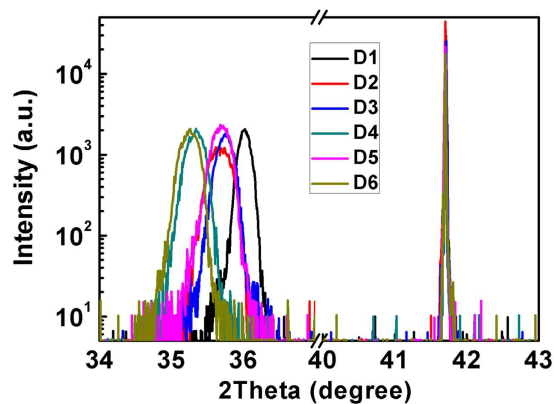


Figure 2. XRD spectra of AlGaN films.

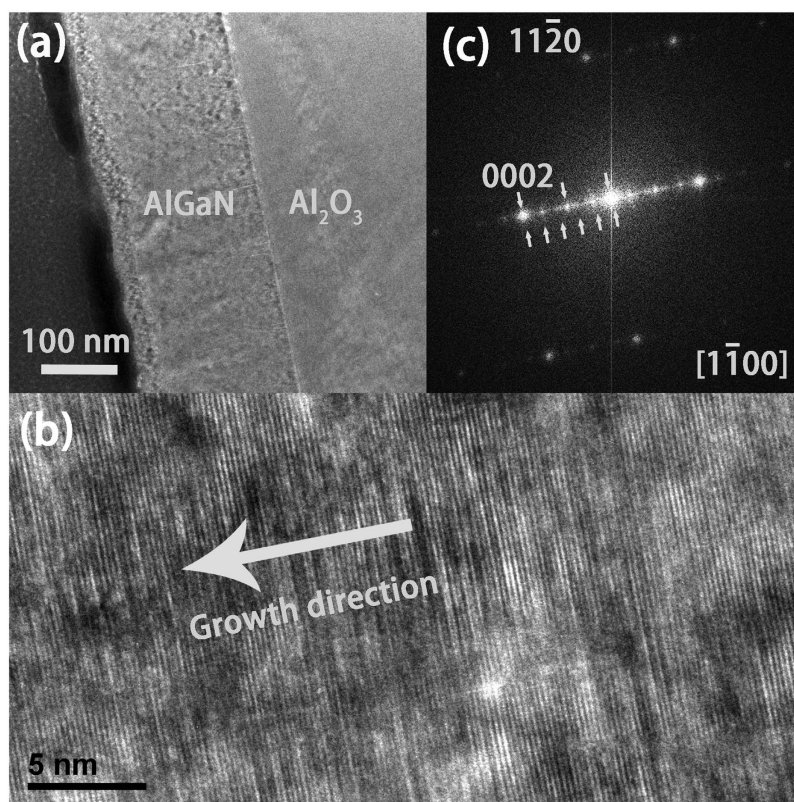
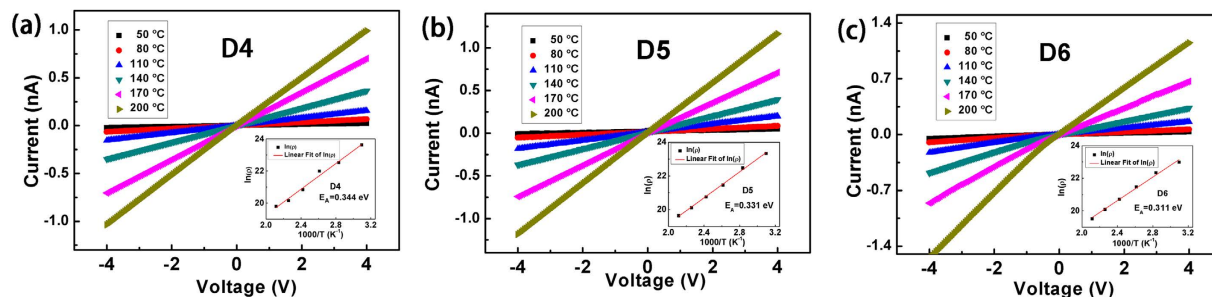


Figure 3. (a) Cross-sectional HRTEM image of AlGaN/Al<sub>2</sub>O<sub>3</sub> in sample D5. (b) The magnified HRTEM image of AlGaN superlattices in sample D5. (c) FFT image of (b).

and  $c_{\text{AlN}}$  of 0.4981 nm. In this way, the compositions of all samples from D1 to D6 were Al<sub>0.97</sub>Ga<sub>0.03</sub>N, Al<sub>0.75</sub>Ga<sub>0.25</sub>N, Al<sub>0.79</sub>Ga<sub>0.21</sub>N, Al<sub>0.53</sub>Ga<sub>0.47</sub>N, Al<sub>0.76</sub>Ga<sub>0.24</sub>N and Al<sub>0.47</sub>Ga<sub>0.53</sub>N, respectively. The compositions of (AlN)<sub>m</sub>/(GaN)<sub>n</sub> in D3 and D5 nearly matched to the designed value of 4:1, while those in D4 and D6 nearly approached to the designed 1:1.

As XRD results reveal only the macro compositions of the AlGaN films, the (AlN)<sub>m</sub>/(GaN)<sub>n</sub> SLs were confirmed by HRTEM results. Figure 3(a) shows the cross-sectional HRTEM image of AlGaN SLs grown on sapphire in sample D5. The total thickness of AlGaN SLs were about 210 nm. The magnified HRTEM image of AlGaN SLs and the corresponding FFT image are shown in Fig. 3(b) and (c). The growth direction of AlGaN SLs on sapphire was [0002], in agreement with the XRD results. As shown in Fig. 3(c), five extra diffraction spots were obtained along [0002] axis in one unit. The four quinquesection spots were attributed to the (AlN)<sub>4</sub>/(GaN)<sub>1</sub> SLs, indicating that the monolayer SL structure was achieved and NN Ga atom number increased in sample D5. The one bisection spot might be caused by the dislocations. Hence sample D5 was measured to be (AlN)<sub>4</sub>/(GaN)<sub>1</sub> superlattices, achieving the designed (AlN)<sub>m</sub>/(GaN)<sub>n</sub> SLs structure with increased NN Ga atom number.



**Figure 4.** I-V characteristics of (a) sample D4, (b) sample D5 and (c) sample D6 at different temperatures. The insets show the corresponding Arrhenius plots of the resistivity versus temperature. The ionization energy of Mg in AlGa<sub>x</sub>N in sample D4, D5 and D6 was determined to be 0.344, 0.331 and 0.311 eV, respectively.

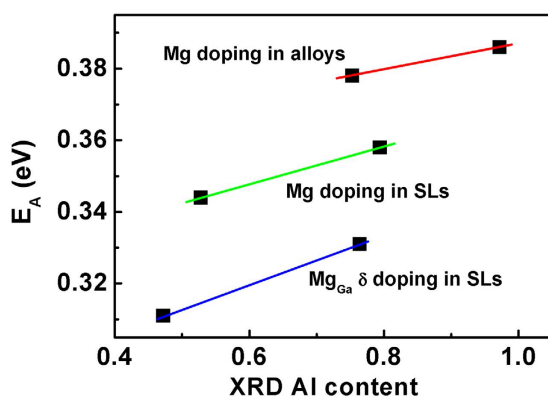


**Figure 5.** The dependence of  $E_A$  on Al composition in Al<sub>x</sub>Ga<sub>1-x</sub>N with three doping methods.

Figure 4 shows the I-V characteristics of sample D4, D5 and D6 at different temperatures. The linear I-V behavior indicated the Ohmic contacts between Ni/Au electrodes and AlGa<sub>x</sub>N films. The good ohmic behavior could be attributed to the formation of p-type NiO<sup>34</sup>. As for sample D5, the resistances were deduced to be 13.67 GΩ, 5.776 GΩ, 2.090 GΩ, 1.042 GΩ, 547.8 MΩ and 340.3 MΩ at temperatures of 50, 80, 110, 140, 170 and 200 °C, respectively. The insets plot the corresponding Arrhenius plot of the resistivity ( $\rho$ ) versus temperature ( $T$ ). Since  $\rho(T) = \rho_0 e^{E_A/kT}$ , the ionization energy ( $E_A$ ) of Mg in Al<sub>x</sub>Ga<sub>1-x</sub>N in sample D5 was fitted to be 0.331 eV as shown in Fig. 4(b). The same procedures were also performed for other samples. As for the asymmetry I-V curves as shown in Fig. 4(c),  $E_A$  was calculated separately under positive and negative voltages and then made of an average. The  $E_A$  for samples D1-D6 were 0.386, 0.378, 0.358, 0.344, 0.331, and 0.311 eV, respectively. The highest  $E_A$  as 0.386 eV was in sample D1 and the lowest  $E_A$  as 0.311 eV lied in sample D6, in match with calculated results that high  $E_A$  in high Al component alloys, and low  $E_A$  in low Al component SLs.

Figure 5 shows the dependence of  $E_A$  on Al composition in AlGa<sub>x</sub>N with three doping methods. Obviously, the  $E_A$  reaches the lower values in Mg<sub>Ga</sub> δ doped AlGa<sub>x</sub>N SLs, the medium in Mg doped SLs and the higher in traditional Mg doped AlGa<sub>x</sub>N alloys. As for Al content around 0.8, the  $E_A$  decreases from 0.378 to 0.358, then to 0.331 eV by the three methods in turn as Mg doped AlGa<sub>x</sub>N alloys, Mg doped SLs and Mg<sub>Ga</sub> δ doped SLs. Hence, Mg acceptor activation energy can be significantly reduced from 0.378 to 0.331 eV by using Mg<sub>Ga</sub> δ doping in (AlN)<sub>4</sub>/(Ga<sub>2</sub>N)<sub>1</sub> SLs instead of traditional Mg doping in Al<sub>0.8</sub>Ga<sub>0.2</sub>N alloys. The difference between the theoretical value (0.26 eV) and the experimental one (0.331 eV) is attributed to two reasons: firstly, the macro function of Mg activation energy in Ga and Al was measured in this experiment while only the Mg activation energy in Ga was calculated to be 0.26 eV; secondly, the as-grown (AlN)<sub>4</sub>/(Ga<sub>2</sub>N)<sub>1</sub> SLs were not perfect single crystal with dislocations which might affect the Mg activation energy. Therefore, we have experimentally proved the theoretical prediction that Mg acceptor activation energy can be significantly decreased in (AlN)<sub>m</sub>/(Ga<sub>2</sub>N)<sub>n</sub> SL<sup>1</sup>.

## Conclusions

In conclusion, we have systematically studied Mg doping in high Al-content AlGa<sub>x</sub>N by using different doping methods. For high Al-content AlGa<sub>x</sub>N, Mg acceptor activation energy can be significantly reduced from 0.378 to 0.331 eV by using Mg<sub>Ga</sub> δ doping in (AlN)<sub>4</sub>/(Ga<sub>2</sub>N)<sub>1</sub> SLs instead of traditional Mg doping in Al<sub>0.8</sub>Ga<sub>0.2</sub>N alloys. Our experimental study verifies the prediction of the first-principles calculations<sup>1</sup>, and provides potential applications in AlGa<sub>x</sub>N-based DUV optoelectronic devices.



## References

- Zhong, H. X. *et al.* Reducing Mg acceptor activation-energy in  $\text{Al}_{0.83}\text{Ga}_{0.17}\text{N}$  disorder alloy substituted by nanoscale  $(\text{AlN})_z/(\text{GaN})_1$  superlattice using  $\text{Mg}_{\text{Ga}}$   $\delta$ -doping: Mg local-structure effect. *Sci. Rep.* **4**, 6710 (2014).
- Zhao, S. *et al.* Aluminum nitride nanowire light emitting diodes: Breaking the fundamental bottleneck of deep ultraviolet light sources. *Sci. Rep.* **5**, 8332 (2015).
- Yang, W. *et al.* High density GaN/AlN quantum dots for deep UV LED with high quantum efficiency and temperature stability. *Sci. Rep.* **4**, 5166 (2014).
- Huang, K. *et al.* Top- and bottom-emission-enhanced electroluminescence of deep-UV light-emitting diodes induced by localized surface plasmons. *Sci. Rep.* **4**, 4380 (2014).
- Al Tahtamouni, T. M., Sedhain, A., Lin, J. Y. & Jiang, H. X. Growth and photoluminescence studies of a-plane  $\text{AlN}/\text{Al}_x\text{Ga}_{1-x}\text{N}$  quantum wells. *Appl. Phys. Lett.* **90**, 221105 (2007).
- Kneissl, M. *et al.* Advances in group III-nitride-based deep UV light-emitting diode technology. *Semicond. Sci. Technol.* **26**, 014036 (2011).
- Gao, N. *et al.* Surface-plasmon-enhanced deep-UV light emitting diodes based on AlGa<sub>N</sub> multi-quantum wells. *Sci. Rep.* **2**, 816 (2012).
- Nakarmi, M. L., Kim, K. H., Zhu, K., Lin, J. Y. & Jiang, H. X. Transport properties of highly conductive n-type Al-rich  $\text{Al}_x\text{Ga}_{1-x}\text{N}$  ( $x \geq 0.7$ ). *Appl. Phys. Lett.* **85**, 3769 (2004).
- Al Tahtamouni, T. M., Sedhain, A., Lin, J. Y. & Jiang, H. X. Si-doped high Al-content AlGa<sub>N</sub> epilayers with improved quality and conductivity using indium as a surfactant. *Appl. Phys. Lett.* **9**, 092105 (2008).
- Yan, Y., Li, J., Wei, S. & Al-Jassim, M. M. Possible approach to overcome the doping asymmetry in wideband gap semiconductors. *Phys. Rev. Lett.* **98**, 135506 (2007).
- Nam, K. B., Nakarmi, M. L., Li, J., Lin, J. Y. & Jiang, H. X. Mg acceptor level in AlN probed by deep ultraviolet photoluminescence. *Appl. Phys. Lett.* **83**, 878 (2003).
- Nakarmi, M. L., Nepal, N., Lin, J. Y. & Jiang, H. X. Photoluminescence studies of impurity transitions in Mg-doped AlGa<sub>N</sub> alloys. *Appl. Phys. Lett.* **94**, 091903 (2009).
- Simon, J., Protasenko, V., Lian, C., Xing, H. & Jena, D. Polarization-Induced Hole Doping in Wide-Band-Gap Uniaxial Semiconductor Heterostructures. *Science* **327**, 60 (2010).
- Gao, L., Xie, F. & Yang, G. Numerical study of polarization-doped AlGa<sub>N</sub> ultraviolet light-emitting diodes. *Superlatt. Microstruct.* **71**, 1 (2014).
- Wu, R. Q. *et al.* Enhancing hole concentration in AlN by Mg:O codoping: Ab initio study. *Phys. Rev. B* **77**, 073203 (2008).
- Aoyagi, Y., Takeuchi, M., Iwai, S. & Hirayama, H. High hole carrier concentration realized by alternative co-doping technique in metal organic chemical vapor deposition. *Appl. Phys. Lett.* **99**, 112110 (2011).
- Aoyagi, Y., Takeuchi, M., Iwai, S. & Hirayama, H. Formation of AlGa<sub>N</sub> and Ga<sub>N</sub> epitaxial layer with high p-carrier concentration by pulse supply of source gases. *AIP Advances* **2**, 012177 (2012).
- Al Tahtamouni, T. M., Lin, J. Y. & Jiang, H. X. Effects of Mg-doped AlN/AlGa<sub>N</sub> superlattices on properties of p-GaN contact layer and performance of deep ultraviolet light emitting diodes. *AIP Advances* **4**, 047122 (2014).
- Nakarmi, M. L., Kim, K. H., Li, J., Lin, J. Y. & Jiang, H. X. Enhanced p-type conduction in Ga<sub>N</sub> and AlGa<sub>N</sub> by Mg- $\delta$ -doping. *Appl. Phys. Lett.* **82**, 3041 (2003).
- Chen, Y. *et al.* High hole concentration in p-type AlGa<sub>N</sub> by indium-surfactant-assisted Mg-delta doping. *Appl. Phys. Lett.* **106**, 162102 (2015).
- Nakarmi, M. L. *et al.* Electrical and optical properties of Mg-doped  $\text{Al}_{0.7}\text{Ga}_{0.3}\text{N}$  alloys. *Appl. Phys. Lett.* **86**, 092108 (2005).
- Kinoshita, T., Obata, T., Yanagi, H. & Inoue, S. I. High p-type conduction in high-Al content Mg-doped AlGa<sub>N</sub>. *Appl. Phys. Lett.* **102**, 012105 (2013).
- Schubert, E. F., Grieshaber, W. & Goepfert, I. D. Enhancement of deep acceptor activation in semiconductors by superlattice doping. *Appl. Phys. Lett.* **69**, 3737 (1996).
- Kozodoy, P., Hansen, M., DenBaars, S. P. & Mishra, U. K. Enhanced Mg doping efficiency in  $\text{Al}_{0.2}\text{Ga}_{0.8}\text{N}/\text{GaN}$  superlattices. *Appl. Phys. Lett.* **74**, 3681 (1999).
- Goepfert, I. D., Schubert, E. F., Osinsky, a., Norris, P. E. & Faleev, N. N. Experimental and theoretical study of acceptor activation and transport properties in p-type  $\text{Al}_x\text{Ga}_{1-x}\text{N}/\text{GaN}$  superlattices. *J. Appl. Phys.* **88**, 2030 (2000).
- Waldron, E. L., Li, Y.-L., Schubert, E. F., Graff, J. W. & Sheu, J. K. Experimental study of perpendicular transport in weakly coupled  $\text{Al}_x\text{Ga}_{1-x}\text{N}/\text{GaN}$  superlattices. *Appl. Phys. Lett.* **83**, 4975 (2003).
- Waldron, E. L., Graff, J. W. & Schubert, E. F. Improved mobilities and resistivities in modulation-doped p-type AlGa<sub>N</sub>/Ga<sub>N</sub> superlattices. *Appl. Phys. Lett.* **79**, 2737 (2001).
- Kauser, M. Z., Osinsky, a., Dabiran, a. M. & Chow, P. P. Enhanced vertical transport in p-type AlGa<sub>N</sub>/Ga<sub>N</sub> superlattices. *Appl. Phys. Lett.* **85**, 5275 (2004).
- Wang, L. *et al.* Strain modulation-enhanced Mg acceptor activation efficiency of  $\text{Al}_{0.14}\text{Ga}_{0.86}\text{N}/\text{GaN}$  superlattices with AlN interlayer. *Appl. Phys. Lett.* **96**, 061110 (2010).
- Wang, W. *et al.* High quality n-type aluminum gallium nitride thin films grown by interrupted deposition and *in-situ* thermal annealing. *Mat. Sci. Semicon. Proc.* **30**, 512 (2015).
- Taniyasu, Y. & Kasu, M. Polarization property of deep-ultraviolet light emission from c-plane AlN/GaN short-period superlattices. *Appl. Phys. Lett.* **99**, 251112 (2011).
- Jiang, X.-h. *et al.* Enhancement of TE polarized light extraction efficiency in nanoscale  $(\text{AlN})_m/(\text{GaN})_n$  ( $m > n$ ) superlattice substitution for high Al content AlGa<sub>N</sub> disorder alloy: ultra-thin Ga<sub>N</sub> layer modulation. *New J. Phys.* **16**, 113065 (2014).
- Zheng, T. C. *et al.* Improved p-type conductivity in Al-rich AlGa<sub>N</sub> using multidimensional Mg-doped superlattices. *Sci. Rep.* **6**, 21897 (2016).
- Ho, J. *et al.* Low-resistance ohmic contacts to p-type Ga<sub>N</sub>. *Appl. Phys. Lett.* **74**, 1275 (1999).

## Acknowledgements

This work is supported by the NSFC under Grant Nos 11574235, 11175135, J1210061 and the MOST China under Grant Nos 2014GB109004. The authors would like to thank Dr. He Zheng, Fan Cao and Ligong Zhao for the technical support.

## Author Contributions

X.W. carried out the experiments and drafted the manuscript. W.W. participated in the design of the study and performed the analysis. J.L.W. participated in the measurements. H.W. conceived the study and participated in its design. C.L. supervised the overall study and polished the manuscript. All authors read and approved the final manuscript.

## Additional Information

**Competing Interests:** The authors declare no competing financial interests.

**How to cite this article:** Wang, X. *et al.* Experimental evidences for reducing Mg activation energy in high Al-content AlGa<sub>n</sub>N alloy by Mg<sub>Ga</sub> δ doping in (AlN)<sub>m</sub>/(GaN)<sub>n</sub> superlattice. *Sci. Rep.* 7, 44223; doi: 10.1038/srep44223 (2017).

**Publisher's note:** Springer Nature remains neutral with regard to jurisdictional claims in published maps and institutional affiliations.



This work is licensed under a Creative Commons Attribution 4.0 International License. The images or other third party material in this article are included in the article's Creative Commons license, unless indicated otherwise in the credit line; if the material is not included under the Creative Commons license, users will need to obtain permission from the license holder to reproduce the material. To view a copy of this license, visit <http://creativecommons.org/licenses/by/4.0/>

© The Author(s) 2017